Mathematical Modeling and Simulation of Fluidized Bed Gasifier: Application to Indian Coal

Rai, Amit*[+]

Department of Chemical Engineering, Sant Longowal Institute of Engineering & Technology Longowal, Sangrur-148106, Punjab, INDIA

Agarwal, Shardha; Mohanty, Bikash

Department of Chemical Engineering, Indian Institute of Technology Roorkee, Roorkee – 247667, Uttarakhand, INDIA

ABSTRACT: *An Eulerian–Eulerian based two-dimensional mathematical modeling approach for bubbling fluidized bed gasifier using FLUENT has been proposed to transfer energy, momentum, and mass between two phases namely solid and gas together with the application of the kinetic theory of solid particle flow. The modeling equation involves eight homogeneous and five heterogeneous reactions kinetics. The eddy dissipation model of FLUENT has been used to incorporate homogeneous reactions kinetics and a user-defined code has been developed that describes the kinetics of heterogeneous reactions. The simulation result shows that the exit syngas composition is in line with the experimental one and has a maximum error of around 4.05% for CO and 2.68% for hydrogen. This model has been used to study the variation in hydrogen concentration in the syngas to maximize hydrogen production based on different operating and design parameters.*

KEYWORDS*: Bubbling fluidized bed gasifier; Indian coal; CFD modeling; Fluent; Hydrogen Production.*

INTRODUCTION

Energy is the essential and most important aspect of sustainable development, and its demand is continuously increasing day by day. Moreover, with the deterioration in the production of conventional energy sources like liquid and gaseous fuel, energy crises arise in most of the countries in the world including India. So, there is a need to use the sources like coal, gas hydrates, oil sand, etc. for energy production [1]. India has around 253 billion tonnes of coal reserves and holds the third position worldwide for coal production. Thus, out of different fossil fuels, coal has a large stake in fulfilling the energy demand globally and, principally in India, as it has become one of the main sources of electricity production in power plants. Coal meets around 70% of the electricity generation and 60% of the commercial energy demand in India.

The high ash fusion temperature and presence of very high ash content in Indian coals along with current coal-based technologies leads to the problem of lower efficiency and environmental damage [2]. In India, many conventional power plants generate electricity by

***To whom correspondence should be addressed.*
+E-mail: mit.rai123456@gmail.com
1021-9986/2023/1/269-285 17/$/6.07

the combustion of coal in low-efficiency combustors, where about two-thirds of the coal energy is lost to the environment and only about one-third is utilized in energy production along with the emission of toxic and harmful gases like CO_2, SO_2, etc. that makes an adverse impact on human health [3]. A coal gasification plant exhibits a better emission profile than a conventional power plant and thus comes under clean coal technology. Out of different coal gasification processes, entrained flow gasifiers are not amenable to the Indian coal condition. Only moving bed and fluidized bed gasifiers can handle high ash coal. A large amount of oxidation products is mainly generated by moving bed gasifier. However, gaseous products are mainly generated by the fluidized bed gasifier because of volatile components in the coal particles. However, these components get cracked in the system, which facilitates easier operation and generates environment-friendly products. Further, a better heat transfer rate is achieved in fluidized bed reactors due to the fluid-like behaviour of the reactants. This gasifier also offers an excellent opportunity in terms of the economics of the process. Moreover, the coal gasification process has become one of the most promising technology due to its capability to produce electricity as well as hydrogen without much loss of energy and pushed the low number of pollutants to the environment as well [2]. Further, hydrogen is becoming one of the most attractive and alternative energy sources of the future in which power generation systems and fuel cell automobiles will play a predominant role and hydrogen production processes must be getting momentum.

The development of modeling equations for fluidized-bed gasification is based on two approaches. The first approach (Lagrangian) is practically viable for the modeling of low solid-phase volume fractions and continuous fluidized beds. The aforementioned method is used to explain the dispersion of the solid phase along with the fundamental conservation laws. The second approach is mainly used for bubbling fluidized beds, where the bed is fluidized to a constant height or high solid-phase volume fractions.

The modeling and numerical solution of bubbling fluidized beds are also based on two methods: the first is the discrete element method, in which each particle is considered by using empirical coefficients of restitution, friction, stiffness, and damping. However, in practical situations, millions of particles are involved hence required large computational resources and enough computation time. In light of this problem, another method based on the Eulerian-granular method as an extension of the Eulerian-Eulerian model that proposed the mechanism to handle the granular flow (fluid-solid) is widely used. The model considers the solution of enthalpy, momentum, continuity, and species equation for each phase. The different forces like virtual lift and drag forces are considered for the interaction of between the flow fields of phases. This model can handle large volume fractions of individual phases that reduce the computational resources and time, as well as allow the detailed analysis of the bubbling fluidized bed [4,5]. The similar work for coal gasification modeling and simulation with fixed, fluidized, and entrained flow gasifiers as well as the application of different operating conditions to increase the hydrogen gas production from the gasifier has been reported by various investigators [6-10]. However, most of the work has been performed for low ash content coals (around 2-5%). The various investigators [4,5,11-16], and many more different authors perform the modeling and parametric based individual study.

There is very little work in the field of CFD modeling along with operating and design-based parametric study to enhance the production of syngas as well as hydrogen from the gasifier for Indian coal as feedstock. The present research work is an effort to address the gaps in the field by developing a CFD model of fluidized bed gasifier through adopting the Eulerian-granular method and testing it for Indian coals as feed material. Further, the present model has been used for operation and design-based parametric study to increase the hydrogen concentration in the syngas from the gasifier.

THEORETICAL SECTION

Computational model

A two-dimensional modeling approach has been implemented to carry out the performance study of bubbling fluidized bed gasifiers within the FLUENT framework. The Eulerian-granular approach is adopted to model the process where two phases exchange momentum, mass, and heat by convection. To decrease the nonlinear characteristics of the model and to obtain good convergence, certain assumptions as postulated by *Cornejo et al.* [4], *Robert et al.* [17], and *Yu et al.* [5] have been taken:(1) The various forces like Brownian, lift, virtual mass, and thermophoretic forces are considered to be negligible. (2) The collision between the different particles

is assumed to be isothermal, i.e. their intensity doesn't vary with temperature and so the fluctuation in solid velocity is not affected by endothermic and exothermic reactions. (3) The temperature of the coal gasification process is less as compared to the combustion process, and so is assumed to be an endothermic process. It is concluded that heat must be required for the gasification process. (4) Two-fluid modeling (solid and gas phase) method has been adopted. The dense and continuous solid phase is to be considered throughout the bed and similarly, the continuous gas phase is to be considered in the freeboard region. To avoid the emission or absorption of radiation energy, the gas phase is also considered the transparent phase. (5) The isothermal, smooth, inelastic, and monodispersed spheres conditions are to be assumed for particles. (6) Coal particles are assumed to be of uniform size and are spherical. (7) it is assumed that instantaneously drying as well as volatilization processes occurs in the gasifier feed region. (8) The de-volatilization process of the coal produces volatiles and char and is assumed to take place instantaneously on entry to the bed. (9) Mass transfer occurs by is molecular diffusion and convection in the two-phase namely bubble and emulsion phase. (10) it is assumed that the No-slip condition occurs for the gas and solid phase. (11) Bubbling mode is considered for the fluidization state of the bed.

Gas solid hydrodynamics

The Eulerian method is used to define both solid and fluid phases that exchange mass, momentum, and energy with each other because the solid phase volume fraction is greater(>11%) in the fluidized bed gasifier. Hence, hydrodynamics of fluidized bed involves the concept of volume fraction that is the volume occupied by each phase. *Cornejo et al.* [4] suggested that the volume of phase q, V, is given by:

$$\mathrm{V_q} = \int (\alpha_\mathrm{q})\,\mathrm{dV} \tag{1}$$

Here,

$$\sum_{q=1}^{n} \alpha_q = 1 \tag{2}$$

The gas and solid phase equation of continuity in terms of volume fractions is given by Eqs. (3) and (4) respectively.

$$\frac{\partial}{\partial \mathrm{t}}(\alpha_\mathrm{g}\rho_\mathrm{g}) + \nabla.(\alpha_\mathrm{g}\rho_\mathrm{g}\mathrm{U_g}) = \mathrm{S_{gs}} \tag{3}$$

$$\frac{\partial}{\partial \mathrm{t}}(\alpha_\mathrm{s}\rho_\mathrm{s}) + \nabla.(\alpha_\mathrm{s}\rho_\mathrm{s}\mathrm{U_s}) = \mathrm{S_{sg}} \tag{4}$$

Here: α is volume fraction, ρ is density, U represents instantaneous velocity, S_{gs} is the gas to the solid phase mass transfer and S_{sg} is solid to gas mass transfer.

The heat, mass, and momentum transfer occur due to the application of the continuity equation along with heterogeneous reactions. In the proposed work, the coal particle reacts with steam, oxygen, CO_2, and hydrogen to convert to the gas phase. Hence, the mass transfer for the phases in Equations (3) and (4) can be given as:

$$\mathrm{S_{sg}} = \mathrm{w_c}\sum \gamma_\mathrm{c}\mathrm{R_c} = -\mathrm{S_{gs}} \tag{5}$$

The ideal gas assumption is used for the gas phase density:

$$\rho_\mathrm{g} = \frac{\mathrm{p}}{\mathrm{RT}\sum_{\mathrm{i=1}}^{\mathrm{n}} \frac{\mathrm{Y_i}}{\mathrm{w_i}}} \tag{6}$$

Where:

p : Pressure of gas

T : mean temperature of the gas mixture

Y_i : Mass fraction for every species

w_i : Molecular weight for each species

The gas-phase momentum equation using volume fraction is given by Eq. (7)

$$\frac{\partial}{\partial \mathrm{t}}(\alpha_\mathrm{g}\rho_\mathrm{g}\mathrm{U_g}) + \nabla.(\alpha_\mathrm{g}\rho_\mathrm{g}\mathrm{U_g}\mathrm{U_g}) = -\alpha_\mathrm{g}\nabla\mathrm{p} - \varphi_{\mathrm{gs}}(\mathrm{U_g} - \mathrm{U_s}) + \nabla.\alpha_\mathrm{g}\tau_\mathrm{g} + \alpha_\mathrm{g}\rho_\mathrm{g}\mathrm{g} + \mathrm{S_{gs}}\mathrm{u_g} \tag{7}$$

Where, φ_{gs} is the momentum exchange coefficient, g is the gravitational constant, $S_{gs}u_s$ is the momentum transfer of the coal.

The stress tensor (τ_g) for gas can be given by Eq. (8)

$$\tau_\mathrm{g} = \mu_{1.\mathrm{g}}(\nabla\mathrm{U_g} + \nabla\mathrm{U_g^T}) - \frac{2}{3}\mu_{1.\mathrm{g}}\nabla.\mathrm{U_g} \tag{8}$$

the solid phase momentum equation is given by Eq. (9):

$$\frac{\partial}{\partial \mathrm{t}}(\alpha_\mathrm{s}\rho_\mathrm{s}\mathrm{U_s}) + \nabla.(\alpha_\mathrm{s}\rho_\mathrm{s}\mathrm{U_s}\mathrm{U_s}) = -\alpha_\mathrm{s}\nabla\mathrm{p} - \nabla\mathrm{p_s} - \varphi_{\mathrm{gs}}(\mathrm{U_s} - \mathrm{U_g}) + \nabla.\alpha_\mathrm{g}\tau_\mathrm{g} + \alpha_\mathrm{g}\rho_\mathrm{g}\mathrm{g} + \mathrm{S_{gs}}\mathrm{u_s} \tag{9}$$

The stress tensor for the solid can be given by Eq. (10):

$$\tau_s = \left(\lambda_s - \frac{2}{3}\mu_s\right)\nabla u_s + \mu_s(\nabla u_s + \nabla u_s^T) \quad (10)$$

Where:λ_s : Bulk viscosity;μ_s : Solid shear viscosity

$$\lambda_s = \frac{4}{3}\alpha_s\rho_s d_s g_o(1-\varepsilon)\left(\frac{\theta_s}{\pi}\right)^{1/2} \quad (11)$$

$$\mu_s = \quad (12)$$

$$^4/_5\,\alpha_s^2\rho_s d_s g_o(1+\varepsilon)\sqrt{\frac{\theta_s}{\pi}}\frac{10\,\rho_s d_s\sqrt{\pi\varphi_s}}{96(1+\varepsilon)\epsilon_s g_s}\left[1+\frac{4}{5g_o\alpha_s(1+\varepsilon)}\right]^2$$

It is observed from momentum equations that relate the drag force in between gas and solid phase are very important for momentum transfer. Hence, the momentum transfer coefficient is calculated by adopting the drag model suggested by *Wen* and *Yu* [18].

$$\varphi_{gs} = \frac{3}{4}C_d\frac{(u_g - u_s)}{d_s}\alpha_g^{-2.65} \quad (13)$$

The drag coefficient C_d is given by:

$$C_d = {}^{24}/_{Re}(1 + 0.15R_e^{0.687}) \text{for } R_e \le 1000 \quad (14)$$

$$= 0.44 \qquad for\ R_e > 1000 \quad (15)$$

Where, Reynolds number, (*Re*), is determined by Eq. (16)

$$Re = \frac{(u_g - u_s)\rho_g d_s}{\mu_g} \quad (16)$$

When the value of solid and gas phase volume fractions is below the maximum allowable value, a granular solid pressure (∇p_s)is approximated by Eq. (9). This pressure term is composed of kinetic and particle collision terms as given in Eq. (17):

$$p_s = \alpha_s\rho_s\theta_s + 2(1+\varepsilon)\alpha_s{}^2 g_o\rho_s\theta_s \quad (17)$$

Where θ_s is the temperature of granular; ε is the particle collision restitution coefficient; g_o – radial distribution function.

The g_o is considered as a correction factor that makes the transition from compressibilitycondition ($\alpha_s < \alpha_{s,max}$,) to incompressibility condition ($\alpha_s < \alpha_{s,max}$,). In the compressibility condition, the spacing between solid particles can decrease continuously whereas in the incompressibility condition no additional decrease can take place. The relationship is given by Eq. (18) is used in the Fluent [4].

$$g_o = \left[1 + \left(\frac{\alpha_s}{\alpha_{s,max}}\right)^{0.33}\right]^{-1} \quad (18)$$

Turbulence model (k-ε per phase):

The turbulent transfer between the gas and solid has a very significant role in the modeling. For the present study, k-ε model turbulence for both phases are selected for the solution of turbulent kinetic energy dissipation rate and turbulent kinetic energy conservation equations and given by Eqs. (19) and (20).

$$\frac{\partial}{\partial t}(\alpha_q\rho_q\overrightarrow{U_q}k_q) = \nabla.\left(\alpha_q\frac{\mu_{t,q}}{\sigma_k}\nabla k_q\right) + \quad (19)$$

$$(\alpha_q G_{k,q} - \alpha_q\rho_q\varepsilon_q) + \sum_{l=1}^{N} K_{lq}\left(C_{lq}k_l - C_{ql}k_q\right) -$$

$$\sum_{l=1}^{N} K_{lq}(\vec{U}_l - \vec{U}_q).\frac{\mu_{t,l}}{\alpha_l\sigma_l}\nabla\alpha_l +$$

$$\sum_{l=1}^{N} K_{lq}(\vec{U}_l - \vec{U}_q).\frac{\mu_{t,q}}{\alpha_q\sigma_q}\nabla\alpha_q$$

$$\frac{\partial}{\partial t}(\alpha_q\rho_q\overrightarrow{U_q}\varepsilon_q) = \nabla.\left(\alpha_q\frac{\mu_{t,q}}{\sigma_\varepsilon}\nabla\varepsilon_q\right) + \quad (20)$$

$$\varepsilon_q/_{k_q}\,[C_{1\varepsilon}\alpha_q G_{k,q} + C_{2\varepsilon}\alpha_q\rho_q\varepsilon_q +$$

$$C_{3\varepsilon}\sum_{l=1}^{N} K_{lq}\left(C_{lq}k_l - C_{ql}k_q\right) - \sum_{l=1}^{N} K_{lq}(\vec{U}_l - \vec{U}_q).\frac{\mu_{t,l}}{\alpha_l\sigma_l}\nabla\alpha_l +$$

$$\sum_{l=1}^{N} K_{lq}(\vec{U}_l - \vec{U}_q).\frac{\mu_{t,q}}{\alpha_q\sigma_q}\nabla\alpha_q$$

The terms

$$C_{lq} = 2, C_{ql} = 2\,{}^{\eta_{lq}}/_{1+\eta_{lq}}, \mu_t = \rho C_\mu\frac{\kappa^2}{\varepsilon} \quad (21)$$

Where ε_q is the dissipations rate and C_μ = 0.09. The term η_{lq} used in above equation is defined as the characteristic time ratio linked to the particle dispersion.

Eulerian-granular model

The Eulerian-granular modeling approach involves random and thermal motion of granular particles and gas molecules and is described by the stress solid phase which accounts for the inelasticity of particles. Granular temperature or pseudo-thermal temperature is used to describe the velocity fluctuations of the particle that describe their kinetic energy. Solid stress acting on the particle is modeled by considering additional acceleration in the particle force balance given by Eq. (22).

$$\frac{du_p}{dt} = F_D(u - u_p) + \frac{g_x(\rho_p - \rho)}{\rho_p} + F_x + F_{interaction} \quad (22)$$

Where $F_{interaction}$ is the additional interaction applying on the particle due to inter-particle interaction and calculated by stress tensor given by Eq. (23):

$$F_{interaction} = -\frac{1}{\rho_p}\nabla.\tau_s \quad (23)$$

The gas-phase velocity fluctuations determine the pressure, stress, and viscosity of the granular solid phase. The velocity fluctuations are described by granular temperature (pseudo thermal temperature) and are proportional to the norm of particle velocity fluctuations.

The transport equation of the Eulerian-granular model can be given as:

$$\frac{3}{2}\frac{\partial(\rho_s\alpha_s\theta_s)}{\partial(t)} + \nabla.(\rho_s\alpha_s v_s\theta_s) = (P_s I + \tau_s):\nabla(v_s) + \nabla.\left(k_{\theta_s}\nabla(\theta_s)\right) - \gamma\theta_s + \varphi_{ls} \quad (24)$$

Where:

$(P_s I + \tau_s):\nabla(v_s)$: Energy generation by the solid stress tensor

$k_{\theta_s}\nabla(\theta_s)$: The energy diffusion

$\gamma\theta_s$: The collisional dissipation of energy

φ_{ls} : The energy transfer between the fluid-solid phase

The k_{θ_s} is given by Equation (25):

$$k_{\theta_s} = \frac{15 d_s\rho_s\alpha_s\sqrt{\theta_s}\pi}{4(41-33\eta)} \times \left[1 + \frac{12}{5}\eta^2(4n-3)\alpha_s g_{o,ss} + \frac{16}{15\pi}(41-33\eta)\eta\alpha_s g_{o,ss}\right] \quad (25)$$

Energy conservation

The following equation describes the solution of energy conservation for each phase:

$$\frac{\partial(\alpha_g\rho_g h_g)}{\partial t} + \nabla.(\alpha_g\rho_g u_g h_g) = -\alpha_g\frac{\partial(P_g)}{\partial t} + \tau_g:\nabla(u_g) - \nabla.q_g + S_g + Q_{sg} + S_{sg}h_{sg} + S_{gs}h_{gs} \quad (26)$$

Where:

q_g : Heat flux

h_{sg} : Enthalpy at the interface

h_g : Gas phasespecific enthalpy

S_g : Chemical reaction source term

Q_{sg} : Intensity of heat transfer intensity between s and q phases

The Eq. (27) represents the rate of heat transfer between two phases (p and q):

$$Q_{pq} = h_{pq}(T_p - T_q) \quad (27)$$

Eq. (27) suggested that the heat transfer rate is temperature-dependent.

Where:

$$h_{pq} = \frac{6k_p\alpha_q\alpha_p Nu_q}{d_p^2} \quad (28)$$

(it is assumed that energy transfer mainly occur by convection)

The value of the Nusselt number is determined by Eq. (29) for porosity in between (0.35 – 1)and Reynolds number (Re) is up to 105.:

$$Nu_q = \left(7 - 10\alpha_p + e{\alpha_p}^2\right)\left(1 + Re_q^{0.2}Pr^{\frac{1}{3}}\right) + \left(1.33 - 2.4\alpha_p + 1.2\alpha_p^2\right)Re_q^{0.7}Pr^{1/3} \quad (29)$$

The *Pr* and *Req* for *qth* phase are given by Eqs. (30) and (31):

$$Pr = \frac{(C_p)_p\mu_p}{\kappa_p} \quad (30)$$

$$Re_q = \frac{\rho_l d_p(v_q - v_l)}{\mu_l} \quad (31)$$

Chemical reactions

In the feed zone, the drying and de-volatilization process occur and so the coal particles get converted into char, volatiles, water vapor, and ash. Char is assumed to be present in the solid state, and so the continuity equation for the solid phase defines the mass balance for char. Proximate analysis of raw coal is used to define the yield of each product.

Coal ⟶ char + volatiles + H_2O + Ash

The present model includes the occurrence of processes like pyrolysis of volatiles, gas-phase reaction, and char reactions inside the gasifier: by the de-volatilization process, the volatiles get converted into the following species:

Table 1: kinetics for heterogeneous reactions.

Chemical reaction	Equations
$3C + 2O_2 \rightarrow CO_2 + 2CO$	$K = 17.9 \exp\left[-13750/T_s\right]$
$C + H_2O \rightarrow CO + H_2$	$K = 0.0000595 \exp\left[-13650/T_s\right]$
$C + CO_2 \rightarrow 2CO$	$K = 3.92 \exp\left[-26927/T_s\right]$
$C + 2H_2 \rightarrow CH_4$	$K = 0.00418 \exp\left[-1.9 \times 10^5/T_s\right]$
$2C + 3H_2 \rightarrow C_2H_6$	$K = 0.00418 \exp\left[-1.9 \times 10^5/T_s\right]$

$$\text{Volatile} \rightarrow v_1CO_2 + v_2CO + v_3H_2 + v_4CH_4 + v_5C_2H_6 + v_6H_2S + v_7NH_3 + v_8\text{tar}$$

Char combustion and gasification

The mechanism of diffusion or the simplified form of the kinetic model can be used to explain the reactions that occur between char particles, steam, and different gases like O_2, H_2O, CO_2, H_2.. However, the concept of an un-reacted core model is used to combine the reaction with diffusion resistance by *Chejne* and *Hernandez* [11] and *Souza-Santos* [19]. *Chen et al.* [20] assumes that, on the surface of char particle reaction between char, O_2, CO_2 and steam takes place with the reaction order of 0.5. the dimension of char particle is assumed to be spherical that is bounded by a stagnant boundary layer. The species present in the gas phase is diffusing through this boundary layer before reacting with char. In the present model, the smaller value of diffusion and kinetic rate control the overall char reaction rate. The kinetic equations for the heterogeneous reactions with Arrhenius parameters are given in Table 1.

Homogeneous reactions

In the control of the turbulent fluctuations fluid flow, the chemical kinetics does not have significant importance in homogeneous rates calculation. Moreover, these are assumed to be affected by turbulence [5]. The kinetic for the homogeneous reactions with Arrhenius parameters are given in Table 2.

Species Transport Equations

The present model considered the mixture of eight chemical species namely carbon monoxide, carbon dioxide, hydrogen, nitrogen, methane, oxygen, steam, and ethane in the gas phase. The conservation equation can be written as Eq. (32) (except for N_2).

$$\frac{\partial(r_g\rho_g Y_{g,i})}{\partial t} + \nabla(r_g\rho_g u_g Y_{g,i}) = -\nabla . r_g J_{g,i} + r_g R_{g,i} + R_{s,i} \quad (32)$$

Where:

$J_{g,i}$: Gas-phase diffusion flux of species ‘i’.

$R_{g,i}$: Net generation rate of species i for a homogeneous reaction

$R_{s,i}$: rate for heterogeneous reaction

Fick’s law given by Equation (33) is applied to determine the molecular flux.

$$J_{g,i} = -\left(\rho_g D_{m,i} + \frac{\mu_t}{\sigma_y}\right)\nabla . Y_{g,i} \quad (\sigma_Y\text{-SchmidtNo.} = 0.7) \quad (33)$$

The mixture diffusion coefficient $D_{m,i}$ is determined by using binary diffusion coefficient:

$$D_{m,i} = \frac{1\text{-}X_i}{\sum_{j\neq 1}\frac{X_j}{D_{i,j}}} \quad (34)$$

Numerical Scheme

The present model uses a two-dimensional unsteady state solver along with their characteristic as shown in Table 3. The boundary conditions related to inlet mass flow andoutlet pressure are used for coal, air inlet, and syngas outlet respectively. The gradient and derivative are evaluated through the green-Gauss cell method with a first-order discretization scheme. A No-slip boundary condition is used for both phases. The upwind method for the discretization of all the conservation equations as well as for transient formulation is used. The quantities of the cell faces are determined by considering that the cell-average value is represented by cell-center values of any field variable, and this value retains for the entire cell. Hence, the equal value of the current face and cell-center of the upstream cell is used in the N-1 iteration.

The green-Gauss cell method is used to evaluate gradients and derivatives. To calculating the value of a scalar φ at the cell center co is given by Eq. (35):

$$(\nabla\varphi)_{co} = \frac{1}{v}\sum_f \overline{\varphi_f}\vec{A_f} \quad (35)$$

Table 2: Kinetics for homogeneous reactions.

Chemical reaction	Equations	Arrhenius equations
$2CO + O_2 \rightarrow 2CO_2$	$R = K[Y_{CO} Y_{O_2}{}^{0.5} \rho_g{}^{1.5}]$	$K = 1 \times 10^{15} \exp\left[-16000/T_g\right]$
$CO + H_2O \rightarrow CO_2 + H_2$	$R = K[Y_{CO} Y_{H_2O}]$	$K = 2780 \exp\left[-1510/T_g\right]$
$CO_2 + H_2 \rightarrow CO + H_2O$	$R = K[Y_{CO_2} Y_{H_2}]$	$K = 0.0265 \exp\left[3968/T_g\right]$
$2H_2 + O_2 \rightarrow 2H_2O$	$R = \frac{K[YH_2{}^{1.5} Y_{O2} \rho_g{}^{2.5}]}{T_g{}^{1.5}}$	$K = 5.159 \times 10^{15} \exp\left[-3430/T_g\right]$
$CH_4 + H_2O \rightarrow CO + 3H_2$	$R = K[Y_{CH_4} Y_{H_2O}]$	$K = 3.12 \times 1 = 10^{10} \exp\left[-12000/T_g\right]$
$C_2H_6 + 2H_2O \rightarrow 2CO + 5H_2$	$R = \frac{K[YC_2H_6 YH_2O \rho_g{}^2]}{T_g}$	$K = 3.12 \times 10^{10} \exp\left[-12000/T_g\right]$
$CH_4 + 2O_2 \rightarrow CO_2 + 2H_2O$	$R = \frac{K[YCH_4 Y_{O2} \rho_g{}^2]}{T_g}$	$K = 3.552 \times 10^{14} \exp\left[-15700/T_g\right]$
$2C_2H_6 + 7O_2 \rightarrow 4CO_2 + 6H_2O$	$R = \frac{K[YC_2H_6 Y_{O2} \rho_g{}^2]}{T_g}$	$K = 3.552 \times 10\text{^}14 \exp\left[-15700/T_g\right]$

Table 3: Computational model parameters used for simulation.

Parameters	Value			
Cells	Quadrilateral			
Particle diameter	0.64 mm			
Grid spacing interval	0.0001 m			
Solver	Unsteady, Ist order implicit			
Multiphase	Eulerian-Eulerian			
Turbulence model	k-epsilon multiphase			
Drag formulation	Syamlal-Obrien			
Pressure velocity coupling	Phase couple simple			
Under relaxation parameters	Pressure	0.3	Body force	0.5
	Momentum	0.6	Density	1
	Volume fraction	0.5	Energy	0.899
	Phase 1		Phase 2	
	CO	0.8	C<solid>	0.5
	O_2	0.8	Volatile	0.6
	CO_2	0.8	H_2O<l>	0.6
	H_2O	0.8		
	Tar	0.8		
	H_2	0.8		
	CH_4	0.8		
Discretization				
Momentum	First-order windup			
Volume fraction	Quick			
Turbulent kinetic energy	First-order windup			
Turbulent energy dissipation	First-order windup			
Time size step	10e-03			
Convergence criteria	1e-05			

The value of φ_f at c_o is determined by Eq. (36):

$$\varphi_f = \frac{(\varphi)_{co} + (\varphi)_{c1}}{2} \quad (36)$$

RESULTS AND DISCUSSION

To validate the proposed model, the experimental values have been collected from the pilot plant as discussed by *Singh et al*. [21]. A schematic diagram of the gasifier along with the fluent geometry is shown in Fig.1.

The geometry of the model was built in Gambit and discretized with 5869 quadrilateral cells. The dimensional specification of the gasifier has already been discussed by *Singh et al*. [21] but for simplicity recreate it here. The total height of the gasifier is 4 m along with 100 mm diameter in the bed zone and 150 mm in the freeboard zone [21]. The coal inlet section has a 40 mm diameter, whereas the pressure outlet section has a 50 mm diameter. The material of construction is high temperature metallic alloy, and the gasifier is equipped with electric heaters to obtain the required temperature at different zones of the gasifier. The granular coal particles are fed with the help of a slow-speed rotary feeder at the rate of around 200 g/min. The air stream is fed through an air distributor that has 120 holes of 2 mm dia. At the inlet of air and steam, a uniform flow condition is assumed. The operating conditions used for model calibration and validation are given in Table 4. The inlet mass flow conditions have been used for coal, air inlets. The boundary conditions related to outlet pressure have been used for syngas. No-slip wall conditions and zero heat flux (adiabatic wall) were used for the gas and solid phase

Validation of model with experimental results

The composition of different species in the syngas obtained from the fluent model along with the experimental result is shown in Table 5.

It is clear From Table 5, that the syngas compositions obtained by the fluent model are in good agreement with the experimental data. The comparison between the predicted and experimental results can also be shown through the bar graph in Fig. 2.

The mole fraction of CO shows a maximum error is 4.05 % and the hydrogen mole fraction isa little bit higher as compared to that of experimental data. This may occur because of the high reaction rate at high temperatures for water-gas shift reactions. Moreover, lower hydrogen combustion rate because of the low availability of oxygen in the gasifier. The contour and profile of temperature distribution in the axial direction are shown in Fig. 3. Simulated results show that the temperature at the outlet of

Table 4: Operating and boundary conditions.

Operating and boundary condition	Value
Operating pressure (Pascal)	500000
Operating temperature (K)	1160.82
Coal feed (kg/hr.)	12
Air supply (LPM)	320
Steam supply (kg/hr.)	2.7
Wall	No-slip

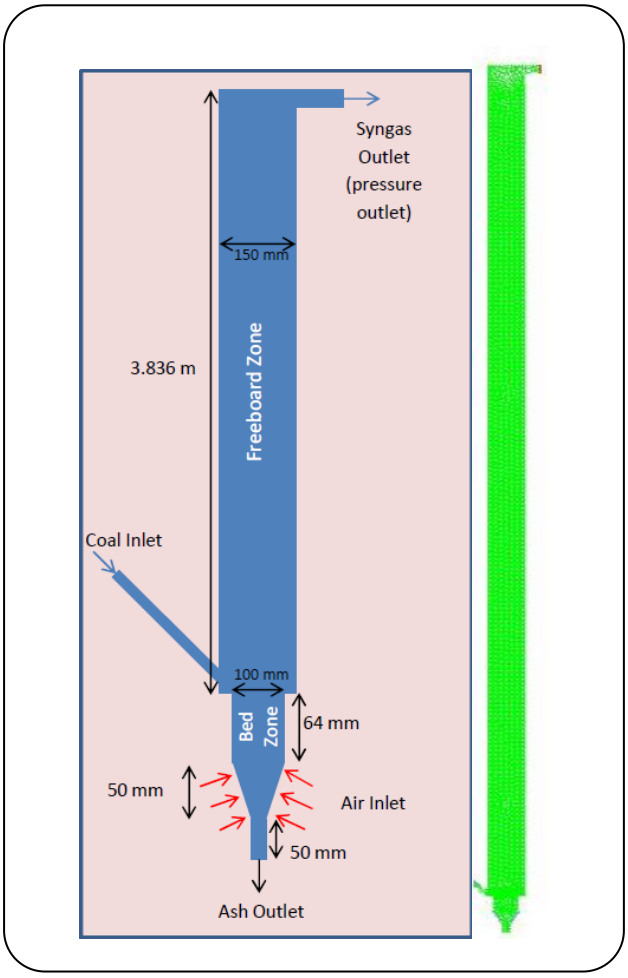

Fig 1: Experimental setup and fluent gasifier geometry.

Table 5: Model validation: predicted values vs. experimental.

Syngas Composition	Predicted Values	Experimental Values	Error (%)
	(Mole Fraction, %)	(Mole Fraction, %)	(%)
CO	17.5	18.24	4.05
CO_2	14.07	14.54	3.23
H_2	19.53	19.02	-2.68
N_2	47.4	47.03	-0.78
CH_4	0.637	0.661	3.63
O_2	0	0	0
H_2O	5.32e-03	0	0
Temperature	1182	1160.82	1.79

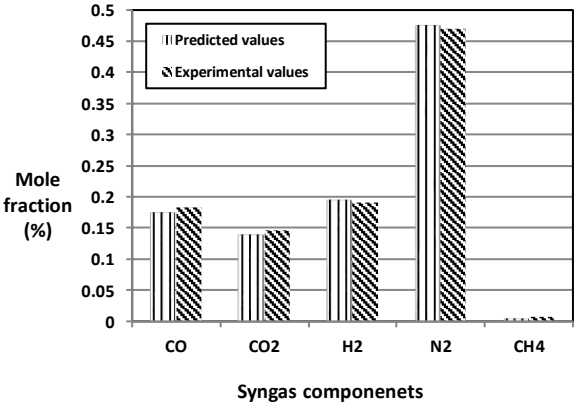

Fig 2: comparison of predicted and experimental results for syngas composition

the gasifier is around 1182 K, which is in good agreement with the experimental result of the temperature of the gasifier of1160.82 K. The temperature profile clearly shows that the temperature decreases in the upward direction and has the higher concentration at the entrance of the gasifier. The reason behind this is that most of the exothermic reactions like char combustion, CO combustion, H_2combustion, CH_4 combustion, C_2H_6 combustion reactions occur mostly at the inlet section of the gasifier due to the availability of plenty of carbon and oxygen. The concentration decreases in the upward direction of the gasifier because of the decrease in the concentration of oxygen as most of the oxygen is consumed near the inlet section by the exothermic reactions. In the upper portion of the gasifier mainly boudouard and endothermic reverse water gas shift reactions may occur, and so the temperature decreases as we move towards the top of the gasifier

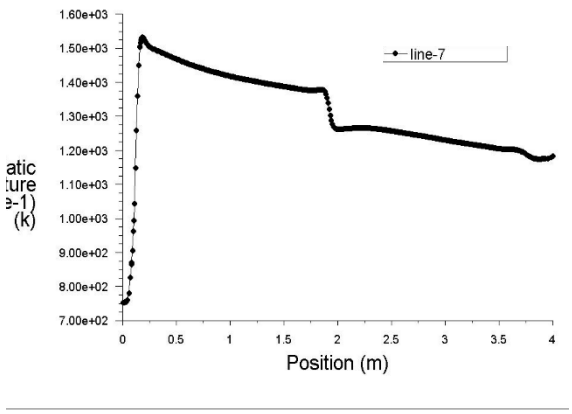

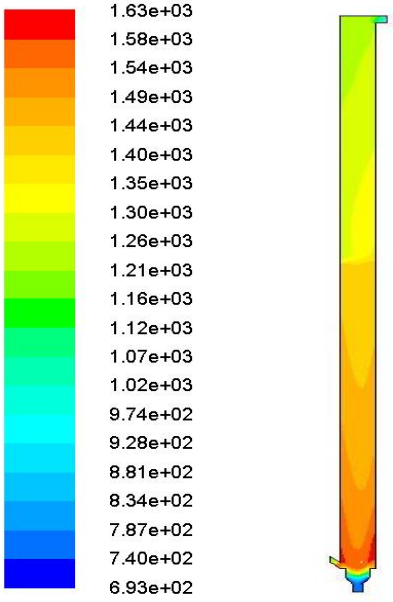

Fig. 3: Profile and contour of axial temperature distribution inside the gasifier.

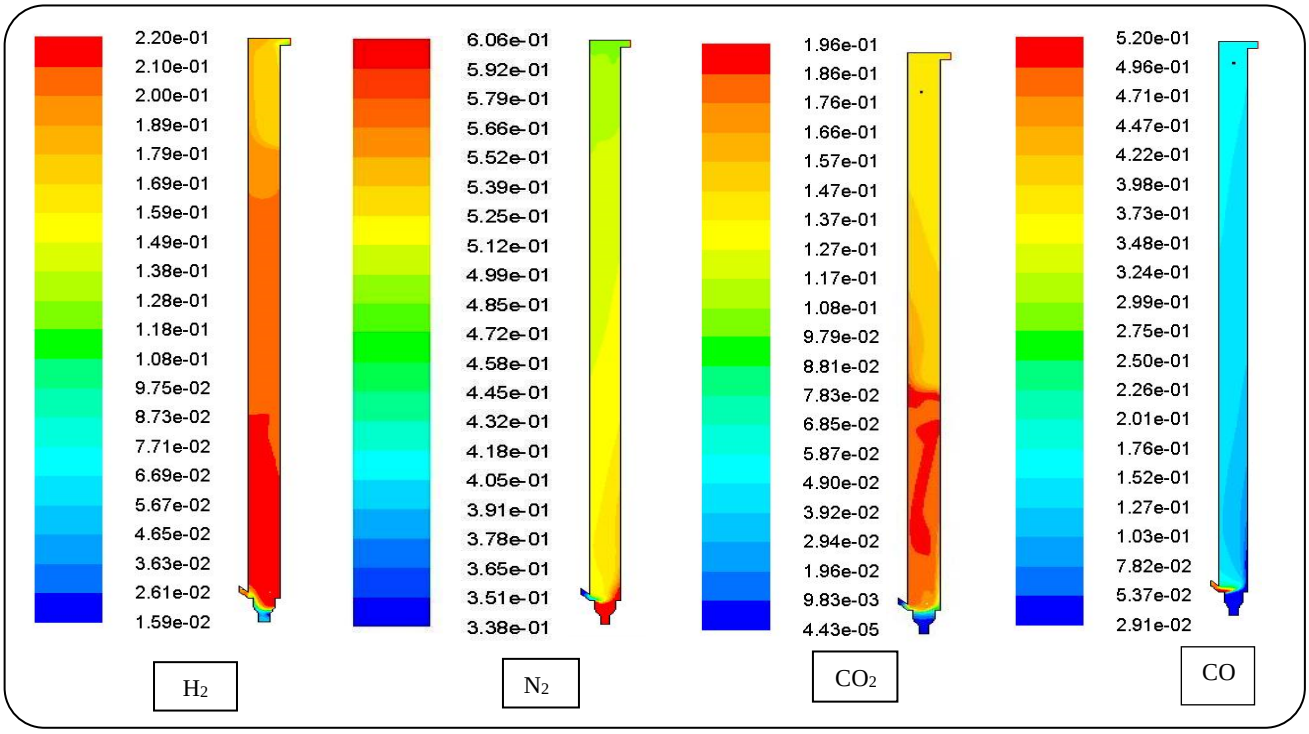

Fig. 4: Species mole fraction distribution.

. Another reason for the decrease of temperature is that the velocity decreases and so the residence time increases resulting in the higher rate of reaction of the endothermic reactions and so the temperature decreases.

Fig. 4 shows the simulated distributions for gas compositions. The composition distribution is strong relative to the temperature profile in the reactor.

CO_2 has a high concentration near the bed region due to char combustion and its concentration decreases towards the top of the gasifier due to reverse water gas shift reaction. The coal volatilization process leads to high CO and H_2 concentration near the bed region. The high temperature near the inlet region of the gasifier leads to a very high rate of water gas shift reaction and its rate decreases towards the top of the gasifier due to a decrease in temperature of the gasifier, so the hydrogen concentration also decreases towards the top of the gasifier.

The concentration of CO increases towards the top of the gasifier because of the occurrence of a reverse water gas shift reaction. After the validation of the modeling equation, the present work aims to increase the hydrogen gas concentration from the gasifier. The variations in different operating and design parameters are included in the present study to analyze hydrogen production. As the composition of char, volatile, ash affects the quality of syngas, so the present study includes the variation in the composition of coal feedstock to examine the effect on syngas production in terms of hydrogen production in the gasifier. The proximate analysis helps to identify variation in the composition of five Indian coal collected from five different Indian coal fields i.e. *Singareni*, *Kushmanda*, *Singrauli*, *Jharia*, *Neyveli*, and results are shown in Table 6

The study for all the Indian coal samples is carried out for the bubbling fluidized bed gasifier having a height of 4m. The syngas from the outlet of the gasifier mainly consists of CO_2, CO,H_2, N_2. The quality of the product gas has a good relationship with the coal properties as well as to the operating conditions. The coal has a high content of volatile matter is more favourable towards pyrolysis. This results in the formation of more hydrogen and hydrocarbon and increases the calorific value of the coal.

The quality of the product gas obtained from the gasifier also depends on the carbon content of coal. As carbon plays an important role in most of the gasification reactions like carbon hydration, water gas shift, boudouard, and other hydro-gasification reactions.

Table 6: Proximate analysis of various Indian coal samples.

Proximate analysis	Singareni	Kushmanda	Singrauli	Jharia	Neyveli
Moisture	9.6	10	12	13	42.52
Volatile matter	23.2	23	20.1	17.51	24.5
Fixed carbon	32.9	25	27.9	28.22	19.5
Ash	34	40.5	40.0	36.08	7.5
Sulfur	0.363	0.28	0.31	0.41	0.63
HHV	4133.3	5590	3641.6	3300	2850

These reactions are mainly responsible for the formation of H_2, CO, CH_4, etc. in the gasifier. Fig. 5 shows the contours of mole fraction of hydrogen for various Indian coals. Fig. 6 shows the contours char of mole fraction of hydrogen for various Indian coals data. It is observed from the figure that the highest fraction of hydrogen comes out to be for Singareni coal data as it has the maximum amount of carbon content as compared to others as well as the higher amount of volatile matter. Hence, the rate of gasification increases along with a higher rate of heat and mass transfer, this increases the hydrogen concentration in the product gas and so the heating value of coal. The minimum amount of hydrogen concentration comes out to before Neyveli coal, as it has less amount of carbon content as well as a very high amount ofmoisture content, so it reduces the rate of gasification reactions and so the hydrogen content in the product gas.

The height of the freeboard region of the gasifier is of significant importance in theproduction of syngas, as most of the gasification reactions like water gas shift reaction, reverse water gas shift reaction, boudouard reaction occur in the freeboard height of the gasifier, and these reactions are the main source for the maximization of hydrogen gas concentration in the syngas. The greater the height of the freeboard region, the higher will be the residence time of the coal particles in the gasifier. So the present study observes the variation in freeboard height of the gasifier from 3-5 m to see the effect on the hydrogen gas production.

Fig.7 illustrates the axial profile of the hydrogen mole fraction for the different free board heights of the gasifier. From the graph, it is clear that, by increasing the freeboard height of the gasifier, hydrogen concentration increases simultaneously, and there is a maximum in the hydrogen gas production for the height of about 4.6 m. The hydrogen concentration may increase because of an increase in the residence time of particles inside the gasifier, and so the combustion and gasification reactions occur more efficiently.

The choice of gasifying medium for coal gasification affects the quality of syngas as well as composition. The process of coal gasification can be performed using air, oxygen, or steam as the gasifying medium. In the present work, the air is used as gasifying agent. At the exit of the gasifier, flue gas contains about 50 vol% nitrogen, together with 8-12 vol% hydrogen, and the rest of the gases as CO, CO_2, CH_4, H_2O, higher hydrocarbons. The product gas can be used only for heat generation or the production of electricity because it has large nitrogen content. As air contains a large percentage of nitrogen (inert gas) in its composition so the product gas has a low heating value (3.5-10 MJ/m^3).

The other gasifying agent that can be used is pure steam. The nitrogen content is lower in the flue gas during steam gasification and the hydrogen content can be as high as 40-55 vol%[22]. Gasification with steam increases the heating value of product gas to 20-35MJ/m^3. The use of steam enhances the rate of those reactions (water-gas shift, steam reforming, char-hydration reaction), which are responsible for the increase of hydrogen gas concentration in the flue gas, which increases the calorific value of product gas. The use of steam improves the overall conversion, energy output, and selectivity of hydrogen.

Fig.8 shows the contour chart and axial profile of the mole fraction of hydrogen present in the syn gas when it is gasified using pure steam. From this figure, it is clear that the use of steam gives hydrogen concentration about 42.9% which is about 54.5% higher as compared to when air plus steam is used. The hydrogen concentration decreases towards the exit of the gasifier because of the reverse water-gas shift reaction. The main drawback associated with

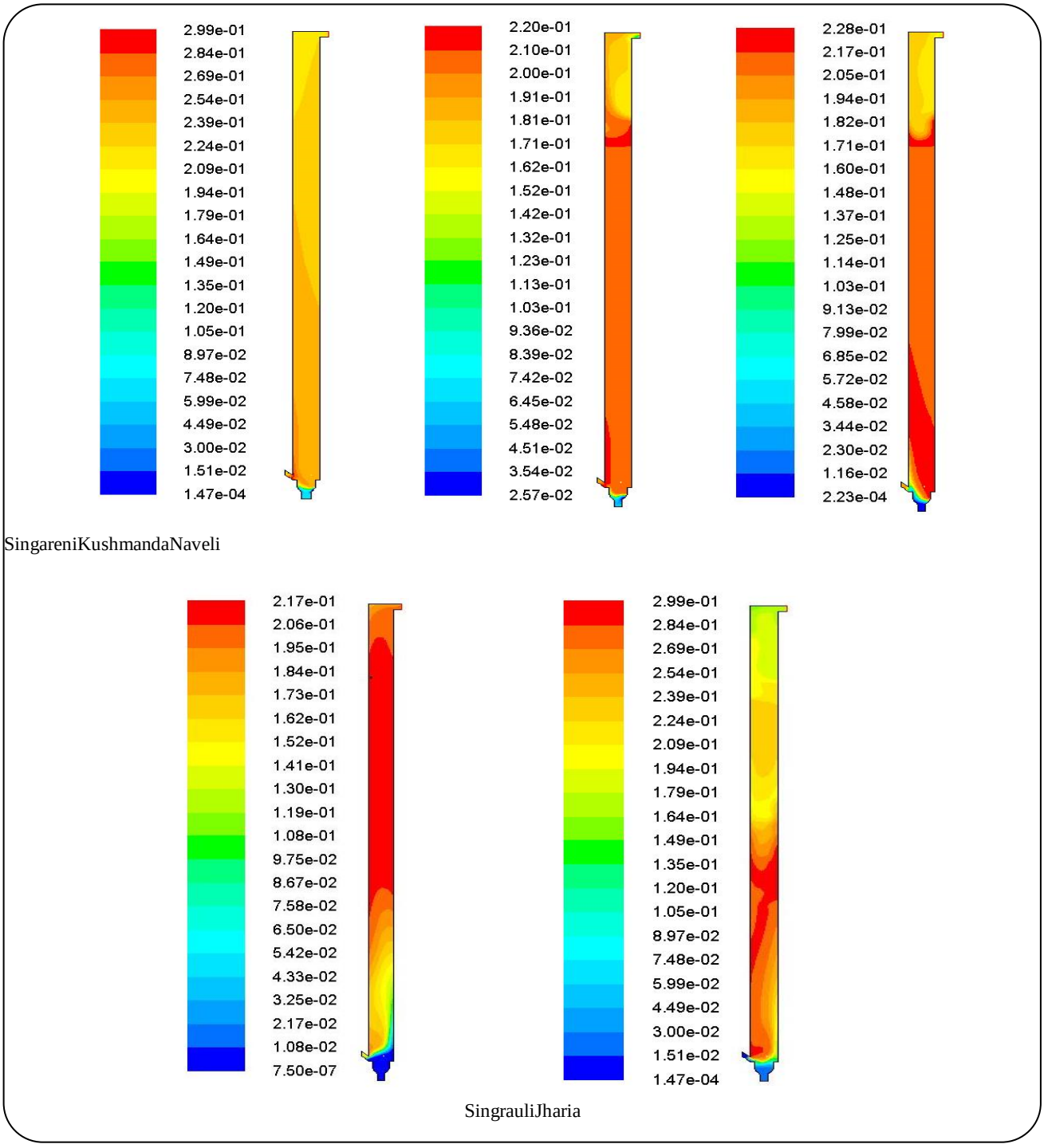

Fig. 5: Contours of species mole fraction of hydrogen for various Indian coals data.

the steam gasification process is the requirement of a high amount of heat due to its endothermic nature.

Fig. 9 shows the axial profile of temperature distribution inside the gasifier when pure steam is used. The use of pure steam as the gasifying agent leads to the rate of exothermic reactions become negligible because of the lack of oxygen in the system, and the endothermic reactions rate increases very rapidly due to the presence of steam in the gasifier, so the temperature inside the gasifier decreases rapidly. The outlet temperature of the gasifier

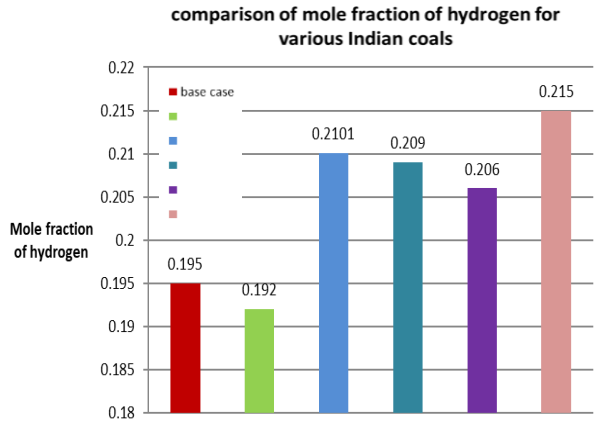

Fig. 6: Comparison of mole fraction of hydrogen for various Indian coals.

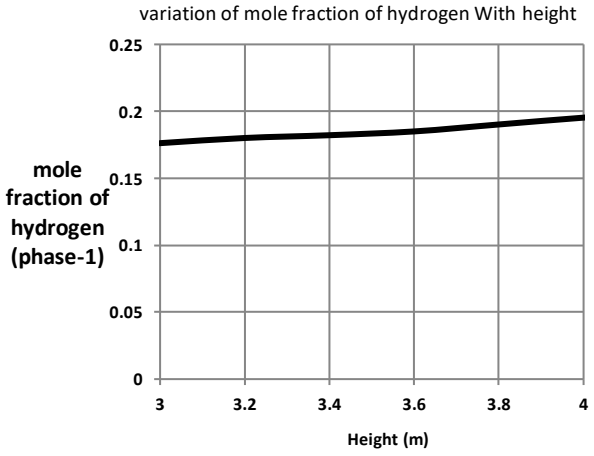

Fig. 7: Variation of mole fraction of hydrogen with height of gasifier.

is found to be around 770 K, whereas the temperature of the pilot plant bubbling fluidized bed gasifier is1182 K. Thus, the use of pure steam increases the hydrogen content in the exit of the gasifier to about 54.5% at the cost of decreasing the temperature of gasifier 412 K. The steam to coal ratio also plays a very significant role in varying the hydrogen gas concentration in syngas. According to *Xiao et al.* [23], with an increase in the value of the ratio, the content of hydrogen and gas heating value first increases and then decreases. Because of the higher value of the ratio, the water gas shift reaction becomes more effective and results in a higher value of hydrogen concentration. But this also provides a dilution effect due to the formation of CO_2 in product gas by the water gas shift reaction. As the product gas is diluted by the higher amount of CO_2 by the addition of steam in the gasifier, the heating value of the product gas decreases [2]. So, the main advantage of varying the steam to coal ratio is to get the optimum value of this ratio at which the concentration of hydrogen is maximized. The present work includes the variation of steam/coal ratio from 0.1 to 2 to seethe effect on the mole fraction of hydrogen.

Fig. 10 shows the variation in mole fraction of hydrogen with steam/coal ratio. From the figure, it is clear that initially by increasing the steam/coal ratio from 0.1 1.0 1.3, the mole fraction of hydrogen increases, and after that, it decreases gradually. The maximum concentration of hydrogen is 55.69 mole% for the steam coal ratio of 1.3. The hydrogen concentration decreases at the higher value of steam/coal ratio due to the dilution effect tprovided by CO_2 in the gasifier as well as due to rapid decrease in the temperature of the gasifier due to endothermic reactions. The use of pure steam as the gasifying agent rapidly decreases the temperature of the gasifier. This reduces the system efficiency as well as the quality of product gas. So, to make the process feasible, there is a need to provide an alternative source of heat to the steam gasification process. This heat can be supplied by burning the fuel in a separate chamber and then supplied to the gasifier with a medium like silica sand. But this type of circulating system is quite complex and expensive in nature. There may be some technical difficulties in the circulation of feedstock processing due to transfer lines or standpipes in the circulating system. So, another solution to provide heat to the gasifier is to add some amount of oxygen to it. This allows the occurrence of exothermic reactions together with the endothermic ones that generate an auto thermal gasification process**.** But the main problem is that the price of oxygen is high so that the overall process could not be economically feasible.

Hence, to increase the temperature of the gasifier, the present study also incorporates the use of (steam plus oxygen) as the gasifying agent. For this purpose, (steam plus oxygen)/coal feedstock ratio is taken as 1.3, because for this ratio of steam/coal maximum amount of hydrogen (55.69%) is obtained. Now the work is based on the variation of steam/oxygen ratio to see the effect on the hydrogen gas concentration as well as on the temperature of the gasifier. Fig.11 shows the

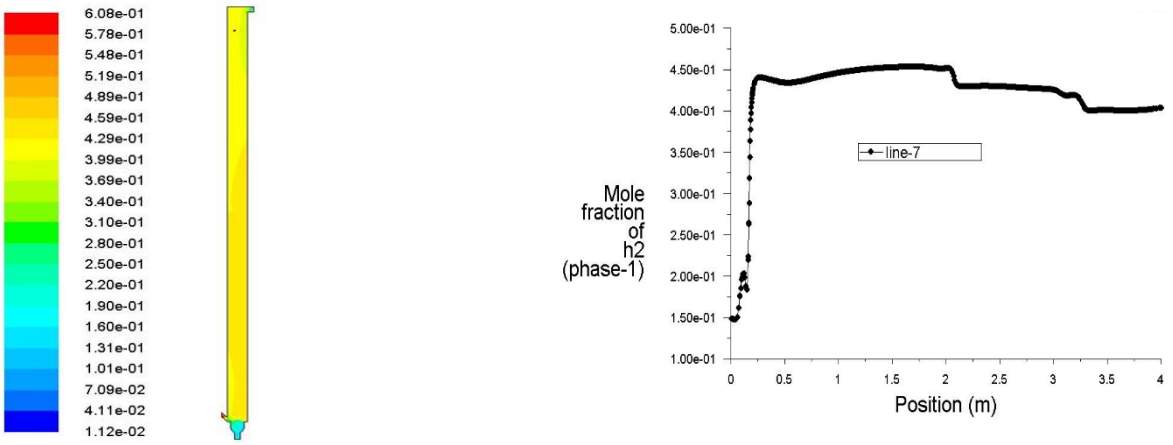

Fig. 8: Contour and axial profile of mole fraction of hydrogen.

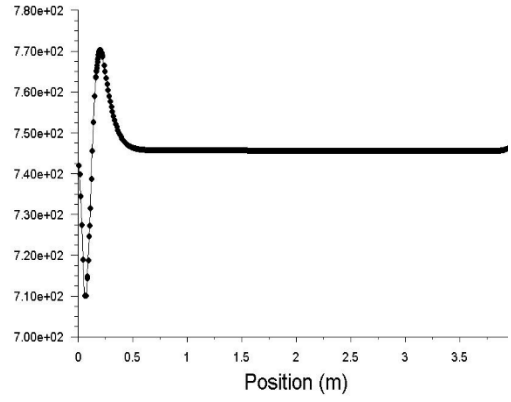

Fig 9: Axial profile of temperature distribution inside the gasifier.

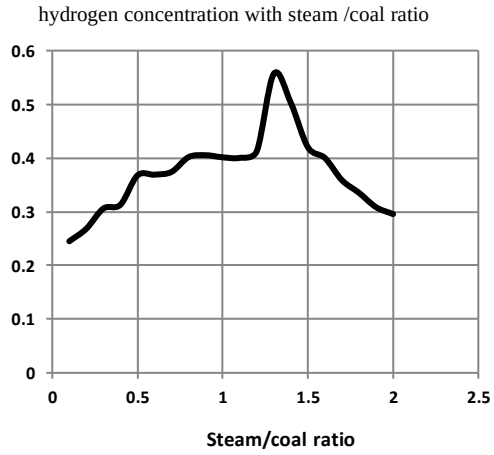

Fig. 10: Variation of mole fraction of hydrogen with steam coal ratio.

variation in mole fraction of hydrogen with steam/oxygen ratio. Steam/oxygen ratio is varied from 0.4 to 0.95. From the figure, it is clear that as the steam/oxygen ratio decreases in the gasifier, hydrogen concentration decreases simultaneously. The reason behind this is the burning of hydrogen inside the gasifier by increasing the oxygen content, that's why less hydrogen is found in the product gas.

Fig. 12 shows the variation of temperature of gasifier with steam/oxygen ratio. From the figure, it is clear that as the oxygen content in the gasifier increases or the steam/oxygen ratio decreases the temperature of the gasifier increases simultaneously. The reason behind this is the occurrence of exothermic reactions inside the gasifier due to the presence of oxygen (char combustion reaction, char hydrogenation reaction, carbon monoxide combustion reaction, water gas shift reaction, hydrogen combustion reaction), and so the temperature of the gasifier increases.

As the overall performance of the gasification process depends on the operating temperature of the gasifier, so it plays a very important role in the overall process of gasification. An increase in the temperature of the gasifier reduces the tar and char content inside the gasifier and so increases the total gas yield, carbon conversion efficiency, mass conversion efficiency, hydrogen yield, and energy output. The increase in all these parameters with the increase in temperature is due to three reasons: first is the initial pyrolysis, second is due to the occurrence of endothermic reactions of char inside the gasifier, and third is due to the occurrence of steam cracking and reforming of the tars, those results in more release of volatile matter

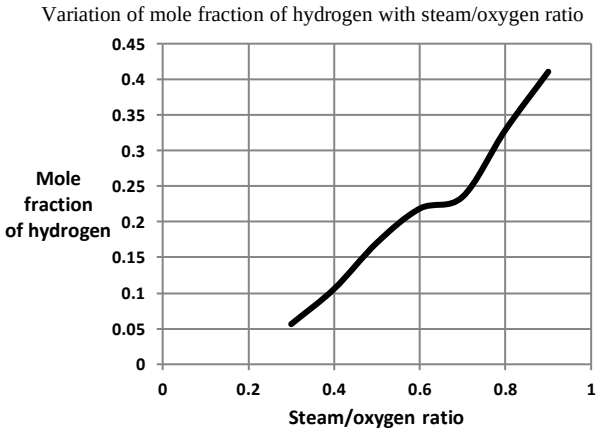

Fig 11: Variation of mole fraction of hydrogen with steam/oxygen ratio.

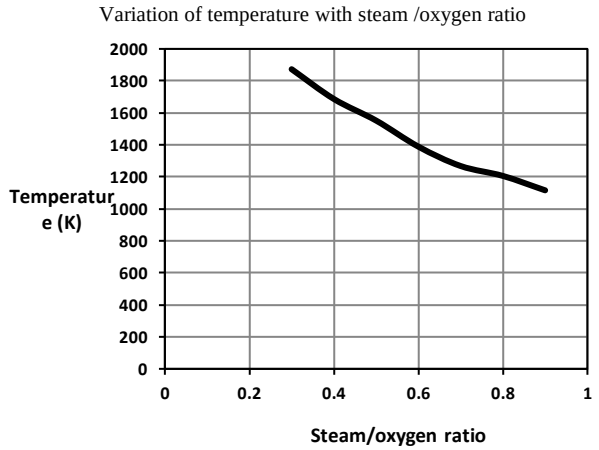

Fig 12: Variation of temperature with steam/oxygen ratio.

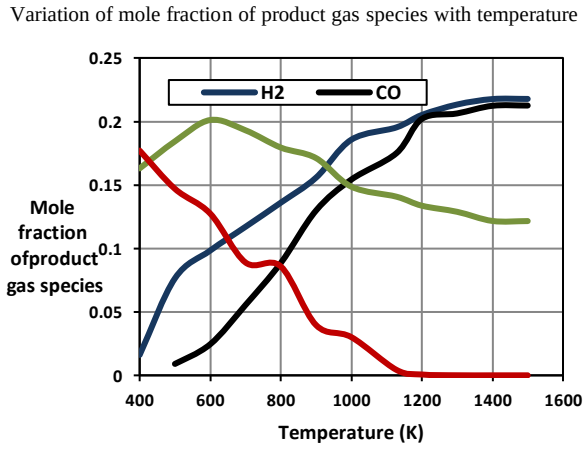

Fig 13: Variation of mole fraction of product gas species with temperature.

to the gasifier. This can also be proved by Le – Chatelier's principle, that at the higher temperature, the endothermic steam reforming reaction dominates. This increases the carbon conversion and hydrogen production in the gasifier.

Fig. 13 shows the variation of mole fraction of product gas species with the increase in gasifier temperature. The gasifier temperature has been varied from 400 to 1500 K to see the effect on product gas species. From the figure, it is clear that, as the temperature of the gasifier increases, the hydrogen and CO concentration tends to increase whereas the concentration of CO_2 and H_2O decreases. The hydrogen concentration in the gasifier increases due to an increase in the rate of steam reforming reaction, char steam combustion reaction, char hydration reaction. Whereas the concentration of CO in the gasifier increases due to a higher rate of reverse water gas shift reaction, boudouard reaction, steam reforming reaction, char hydration reaction. As the temperature of the gasifier increases, the rate of forwarding water gas shift reaction, carbon monoxide combustion reaction, char combustion reaction decreases (exothermic reactions), so the CO_2 content in the gasifier decreases. The hydrogen concentration in the gasifier decreases due to an increase in the rate of char hydration reaction, steam reforming reaction, and decrease in the rate of the hydrogen combustion reaction.

CONCLUSIONS

- The syngas composition obtained from the model of bubbling fluidized bed gasifier is in good agreement within a maximum error of less than $\pm 5\%$ with the experimental data obtained from the pilot plant.
- The temperature data obtained from the modeling of the gasifier validated the experimental data within $\pm$ 1.79% of error.
- Most of the combustion reactions (exothermic nature) like char combustion reaction, char hydrogenation reaction, carbon monoxide combustion reaction, water gas shift reaction, hydrogen combustion reactions occur rapidly near the coal inlet region due to the availability of oxygen and char.
- The model results show that different Indian coal produces different hydrogen gas concentrations in the product gas. The results reveal that as the volatile matter content and carbon content in the coal composition increases, the hydrogen production from the gasifier increases.

•The model is also used to study the effect of temperature on the produced hydrogen gas concentration. By varying the operating temperature from 400 to 1500 K, it is clear that the concentration of hydrogen and carbon monoxide increases while that of carbon dioxide and water decreases.

•The study also includes the use of steam as the gasifying agent to see the effect on hydrogen gas concentration. The obtained hydrogen gas concentration is around 42.9% when pure steam is used as the gasifying agent which is about 54.5% higher as compared to the base case. However, the use of pure steam decreases the temperature of the gasifier due to the dominance of endothermic reactions. The temperature of the gasifier for this case is around 770 K.

•Variation steam to coal ratio affects the hydrogen gas concentration produced from the gasifier. Results reveal that for steam/coal ratio from 0.1 to 1.3 hydrogen concentration increases. However, a further increase in this ratio from 1.3 decreases the hydrogen concentration. The maximum value of hydrogen concentration is for steam/coal ratio of 1.3 and it is around 55.69 mol%.

•The use of pure steam as the gasifying agent decreases the temperature of the gasifier. Hence, to increase the temperature, the mixture of steam and oxygen is used as gasifying agent. The study depicts the variation of steam/oxygen ratio on the hydrogen gas concentration. By varying the steam/oxygen ratio from 0.4 to 0.95, the results reveal that the hydrogen concentration increases.

•Further, the study shows that an increase in the freeboard height of the gasifier increases the hydrogen concentration due to an increase in the residence time of gasification reactions.

Received : Dec. 17, 2021 ; Accepted : Jan. 31, 2022

REFERENCES

[1] Web1 http://www.aspousa.org/index.php/peak-oil-reference/peak-oil-data/(2013, April).

[2] Chavan P., Datta S., Saha S., Sahu G., Sharma T., Influence of High Ash Indian Coals in Fluidized Bed Gasification Under Different Operating Conditions, *Solid Fuel Chem.*,**46**: 108-113 (2011).

[3] Web2. http://www.fossil.energy.gov/programs/powersystems/gasification/(2013, April)

[4] Cornejo P., Farias O., Mathematical Modeling of Coal Gasification in a Fluidized Bed Reactor Using a Eulerian Granular Description, *Int. J. Chem. React. Eng.*,**9 Article A2**: 1-30 (2011).

[5] Yu L., Lu J., Zhang X., Zhang S., Numerical Simulation of Bubbling Fluidized Bed Coal Gasification by the Kinetic Theory of Granular Flow,*Fuel*,**86**: 722-734 (2007).

[6] Chang H., Xiao F., Chu K.H., Li A., Liu Y., Industrial-scale Fixed-bed Coal Gasification: Modeling, Simulation and Thermodynamic Analysis, *Chin. J. Chem. Eng.*,**22**: 522-530 (2014).

[7] Chatterjee P.K., Datta A.B., Kundu K.M., Fluidized Bed Gasification of Coal, *Can. J. Chem. Eng.*,**73**: 204-221 (1993).

[8] Kim Y.J, Lee, J.M., Kim, S. D., Modeling of Coal Gasification in an Internally Circulating Fluidized Bed Reactor with Draught Tube, *Fuel*,**79**: 69-77(2000).

[9] Maurer R., Industrial Fixed-Bed Coal Gasification: An Economic Alternative to Deregulated Natural Gas, SAE Technical Paper, 810995 (1981).

[10] Zhang Y., Zheng Y., Co-Gasification of Coal and Biomass in a Fixed Bed Reactor with Separate and Mixed Bed Configurations, *Fuel*,**183**: 132-138 (2016).

[11] Chejne F., Hernandez J.P., Modeling and Simulation of Coal Gasification Process in Fluidized Bed,*Fuel*,**81**: 1687-1702 (2002).

[12] Gera D., Gautam M., Tsuji Y., Kawaguchi T., Tanaka T., Computer Simulation of Bubbles in Large Particle Fluidized Beds, *Powder Tech.*,**98**: 38-47 (1998).

[13] Hamel S., Krumn W., Mathematical Modeling and Simulation of Bubbling Fluidized Bed Gasifiers, *Powder Tech.*,**120**: 105-112 (2001).

[14] Ross D.P., Yan H.M., Zhong Z., Zhang D.K., A Non-Isothermal Model of a Bubbling Fluidized Bed Coal Gasifier, *Fuel*,**84**: 1469-1481 (2005).

[15] Xie J., Zhong W., Jin B., Shao Y., Huang Y., Eulerian- Lagrangian method for Three-Dimensional Simulation of Fluidized Bed Coal Gasification, *Adv. powder Tech.*,**24**: 382-392 (2013).

[16] Yan H.M., Heidenreich C., Zhang D.K., Mathematical Modeling of a Bubbling Fluidized Bed Coal Gasifier and the Significance of Net Flow, *Fuel*,**77**: 1067-1079 (1998).

[17] Robert P.M.A., Richard M.F., James K.F., Modeling of Pilot Scale Fluidized Bed Coal Gasification Reactor, *Fuel Proc. Tech.*,**19**: 265-290 (1988).

[18] Wen C.Y., Yu Y.H., Mechanics of Fluidization, *Chem. Eng. Prog. Symp. Series*,**62**: 100–11 (1966).

[19] De Souza-Santos M.L., Comprehensive Modeling and Simulation of fluidized Bed Boilers and Gasifiers,*Fuel*,**68**: 1507–21 (1989).

[20] Chen G., Spliethoff H., Andries J., Glazer M., Biomass Gasification in a Circulating Fluidized Bed Part I: Preliminary Experiments and Modeling Developments, *Energy Sources*,**26**: 485-498 (2004).

[21] Singh G.K., Mohanty B., Mondal P., Chavan P., Datta S., Modeling and Simulation of a Pilot-Scale Bubbling Fluidized Bed Gasifier for the Gasification of High Ash Indian Coal Using Eulerian-Granular Approach, *Int. J. Chem. Reac. Eng.*,**14**: 417–431 (2016).

[22] Gil J., Aznar M.P., Caballero M.A., Frances E., Corella J., Biomass Gasification in Fluidized Bed at Pilot Scale with Steam Oxygen Mixture. Product Distribution for Very Different Operating Conditions, *Energy and Fuels*,**11**: 1109-1118 (1996).

[23] Xiao R., Zhang M., Jin B., Huang Y., High Temperature Air/Steam Blown Gasification of Coal in a Pressurized Spout Fluid Bed, *Energy Fuels*,**20**: 715-720 (2006).